ELSEVIER

Chemical Engineering Journal 125 (2007) 139–147

Chemical Engineering Journal

www.elsevier.com/locate/cej

Kinetic modeling of steam reforming of ethanol for the production of hydrogen over Co/Al_2O_3 catalyst

D.R. Sahoo, Shilpi Vajpai, Sanjay Patel, K.K. Pant *

Department of Chemical Engineering, Indian Institute of Technology-Delhi, Hauz Khas, New Delhi-110016, India

Received 5 May 2006; received in revised form 2 August 2006; accepted 7 August 2006

Abstract

The kinetics study of steam reforming of ethanol was done using Co/Al_2O_3 catalysts to investigate the effect of reaction temperature, contact-time and steam to ethanol molar ratio on hydrogen production. Co/Al_2O_3 catalysts, prepared by wet impregnation method, were characterized for their surface area, pore volume, pore size and X-ray diffraction pattern. All the experiments were carried out in a fixed-bed tubular reactor. Surface reaction mechanism has been proposed based on the literature and product distribution obtained in the present study. The mechanistic kinetic model using Langmuir–Hinshelwood (L–H) approach was developed considering surface reaction mechanisms of steam reforming of ethanol, water gas shift and ethanol decomposition reactions. The kinetic parameters of the multi-response non-linear mechanistic kinetic model were estimated using a non-linear least-square regression by fitting the expression to the experimental data. A reasonably good fit of the data indicates that the formation of acetaldehyde from ethoxy is the rate-determining step (RDS) for reforming reaction. The kinetic model is able to describe the steam reforming of ethanol process adequately for a wide range of experimental data.

Keywords: Ethanol steam reforming; Hydrogen; Kinetics; Co/Al_2O_3 catalyst

1. Introduction

Presently, nearly all the energy requirements are derived directly or indirectly from the non-renewable sources such as fossil fuels, which is also associated with release of large quantities of green house gases. The gradual depletion of these fossil fuel reserves and efforts to control pollution, and green house gas emissions has generated a considerable interest in using alternative sources of energy. Fuel cells, using hydrogen as fuel, are considered to have the potential to provide a clean energy source as an alternative to gasoline or diesel engines [1,2]. The hydrogen required for the polymer electrolyte membrane (PEM) fuel cell can be generated from liquid hydrocarbons such as methanol [3], ethanol, dimethyl ether, etc. Among the several possibilities, the production of hydrogen via steam reforming of ethanol (SRE) could favor the use of hydrogen as an alternative fuel. Ethanol presents several advantages related to natural availability, storage, handling and safety [4]. Ethanol can be produced renewably from several bio mass sources, including energy plants, waste material from agro-industries or forestry residue materials, organic fraction of municipal solid waste, etc. The problem with the ethanol reforming process is that, besides the formation of H_2, CO_2 and CH_4, the gaseous fuel produced usually contains high levels of CO, which is poisonous to the Pt anode of PEM fuel cell. Even with the more advanced anode catalysts, the system cannot accept more than 20 ppm for efficient operation [4–6]. Methane and carbon monoxide formation decreased substantially at higher water-to-ethanol ratio in the feed [7,8].

It has been reported that hydrogen, carbon dioxide and carbon monoxide selectivity increases with increase in reaction temperature [9]. Haga et al. [10] studied the catalytic properties of different metal supported on Al_2O_3 for ethanol steam reforming at 673 K and concluded that Co/Al_2O_3 catalysts are more effective for the overall SRE reaction.

$$C_2H_5OH + 3H_2O \leftrightarrow 6H_2 + 2CO_2 \quad \Delta H^\circ = 173.5\,\text{kJ/mol} \tag{1}$$

Batista et al. [11] studied the steam reforming of ethanol over Co/Al_2O_3, Co/MgO and Co/SiO_2 catalysts. Among them, hydrogen selectivity was highest over Co/Al_2O_3 catalyst. They

* Corresponding author. Tel.: +91 11 26596172; fax: +91 11 26581120.
E-mail address: kkpant@chemical.iitd.ac.in (K.K. Pant).

1385-8947/$ – see front matter © 2006 Elsevier B.V. All rights reserved.
doi:10.1016/j.cej.2006.08.011

Nomenclature

C_{S1}^{T}	total surface concentration of site 1 (mol/m$^{2)}$
D	reactor inner diameter (mm)
Dp	catalyst particle size (mm)
E_i	activation energy for rate constant of reaction i (kJ/mol)
ΔH_i	heat of adsorption for surface species i or heat of reaction for formation of surface species i (kJ/mol)
k_i	rate constant for reaction i; units will be specific to the form of the rate expression
k_i^{∞}	pre-exponential rate constant for reaction i (m^2/(mol s))
K_i	equilibrium constant of reaction i or adsorption coefficient for surface species i
L	catalyst bed height (mm)
p_i	partial pressure of component i (atm)
r_i	rate of reaction of component i (mol/s m^2)
ΔS_i	entropy of adsorption for species i (J/(mol K))
T	temperature (K)
X	ethanol conversion (%)

Acronyms

ED	ethanol decomposition
PEM	polymer electrolyte membrane
PID	proportional integral derivative
RDS	rate-determining step
S/E	steam to ethanol molar ratio
SRE	steam reforming of ethanol
W/F	weight of catalyst/molar flowrate of ethanol
WGS	water gas shift
XRD	X-ray diffraction

Subscripts

D	decomposition reaction
r	ethanol steam reforming reaction
S1	active site in reaction mechanism
w	water gas shift reaction

Superscripts

(1)	species adsorbed on active site S1
T	indicating total concentration of active sites

observed negligible amount of oxygenate formation. Limited literature available on steam reforming of ethanol suggests that Co/Al_2O_3 catalysts are effective for hydrogen production. However, details of catalyst preparation and kinetic models are not available. The present work aims at preparation of Co/Al_2O_3 catalyst with varying amount of Co and study the performance of steam reforming of ethanol for high H_2 selectivity. The performance of the catalyst was studied in the temperature range 673–973 K, contact-time 3–17 kg cat./(mol/s), steam to ethanol (S/E) molar ratio 1–8 at atmospheric pressure. The present study also describes the product distribution, product selectivity and yield in order to propose a reaction scheme followed by development of kinetic model for steam reforming of ethanol.

2. Experimental

2.1. Catalyst preparation

A series of Co/Al_2O_3 catalysts, with varying Co loading (10–20 wt.%) on alumina support, were prepared using wet impregnation method. The solution of cobalt nitrate ($Co(NO_3)_2{\cdot}6H_2O$) precursors was made by dissolving cobalt nitrate (Merck, Germany) in distilled water. The alumina pellets (IPCL India) were crushed and sieved to a particle size of 20–25 mesh size, dipped in solution for 2 h and stirred vigorously. The excess water was removed in a rotary vacuum evaporator, followed by drying overnight at 483 K and calcination at 873 K for 6 h.

2.2. Catalyst characterization

Surface area, pore volume and pore size of the catalysts were measured by ASAP 2010 micromeritics USA using nitrogen adsorption–desorption method. Different crystalline phases present in calcined and used catalysts were identified by X-ray powder diffraction (XRD) using Philips X'PERT PW 1827/21 diffractometer. The operation was done with monochromatic Cu Kα 1.5418 Å radiation at a current of 30 mA with diffraction angle ranging from 10° to 60°.

2.3. Activity test for steam reforming of ethanol

Catalysts performance was evaluated in a fixed-bed stainless steel reactor (19 mm i.d.). SRE reaction was carried out at an atmospheric pressure by placing the reactor in an electric furnace consisting of two heating zones equipped with two PID temperature controllers. A thermocouple was placed at the center of catalyst bed to monitor the reactor temperature. Catalysts were tested in an integral mode at different reaction temperatures, contact-times and steam to ethanol molar ratio. Prior to reforming reaction catalysts were exposed to a reduction environment. The reduction was carried out in situ using a stream of 10% hydrogen in nitrogen at a temperature ramp of 10 K/min and dwelling at 773 K for 2 h. The reactor used in this study was operated in a steady state continuous plug-flow mode under isothermal condition. The controlled flow of liquid ethanol and water were passed separately to a vaporizer maintained at 493 K where reactants got vaporized and mixed with the stream of nitrogen. Nitrogen was used as carrier gas and internal standard for the subsequent chromatographic analysis. The reactant mixture fed to the reactor maintained at desired temperature where the steam reforming of ethanol reaction took place. The stream of products and unconverted species passed through a condenser and liquid–gas separator followed by sampling ports. Reaction products were analyzed by Nucon-5700 gas chromatograph, equipped with thermal conductivity detector and carbosphere column for the gaseous product concentration measurement and flame ionization detector with porapak-Q col-

umn for unconverted ethanol and any other liquid hydrocarbon formed during reaction. Preliminary runs were carried out with different catalyst particle size ranging from 0.2 to 1.5 mm to study the effect of particle size on ethanol conversion. Results revealed that the ethanol conversion was almost constant for the particle size 1.0 ± 0.2 mm, indicating that diffusional resistance does not affect the rate. Therefore, average particle size 0.6 corresponds to 20/25 mesh was selected for all the kinetic experiments. Runs were also carried out to achieve the negligible film diffusion effect on kinetic data as suggested by Idem and Bakhshi [12]. Since the SRE process is highly endothermic, catalyst was diluted in the Pyrex quartz beads of same size to achieve the isothermal conditions. The plug flow condition was achieved by eliminating back mixing and channeling by providing catalyst bed height to catalyst particle size, $L/\mathrm{Dp} \geq 50$ and that of internal diameter of reactor to catalyst particle size, $D/\mathrm{Dp} \geq 30$, respectively, based on literature [13,14]. The kinetic data were collected by varying contact-time (W/F) 3–17 kg cat./(mol/s), temperature 673–973 K and steam to ethanol (S/E) ratio 3–8 molar at atmospheric pressure. All the kinetic data were collected (run time of 3–7 h) during which deactivation of catalyst did not observe.

3. Results and discussion

3.1. Catalyst characterization

The surface area, pore volume and pore size of all the prepared Co/Al_2O_3 catalysts are listed in Table 1. The surface area and pore volume of Co/Al_2O_3 catalysts decreased with increasing cobalt loading compared to γ-Al_2O_3 support due to the coverage of pore space. The XRD patterns for calcined fresh and used catalysts are shown in Fig. 1. The Co was present mainly in Co_3O_4 form in fresh calcined catalyst. The spectra of spent catalyst, reduced before reforming, revealed that part of the Co converted to Co_3O_4, CoO and $CoAl_2O_4$ spinal.

3.2. Effect of metal loading on catalytic activity

Co metal has high selectivity towards overall reforming reaction. The variation of ethanol conversion with temperature at constant W/F (17 kg cat./(mol/s)) is shown in Fig. 2 for the three catalysts prepared. The ethanol conversion increased with temperature for all the three catalysts. The 15% Co/Al_2O_3 catalyst gave higher ethanol conversion than 10 and 20% Co/Al_2O_3 catalysts in the range of temperature studied. The Co sites promote the reforming and water gas shift reactions, therefore, as the metal loading increased from 10 to 15% more number of active

Table 1
Physical properties of catalysts

Types of catalyst	S_{BET} (m^2/g)	Pore volume (cm^3/g)	Average pore diameter (Å)
10% Co/Al_2O_3	159	0.36	94.3
15% Co/Al_2O_3	158	0.34	97.5
20% Co/Al_2O_3	138	0.30	82.5

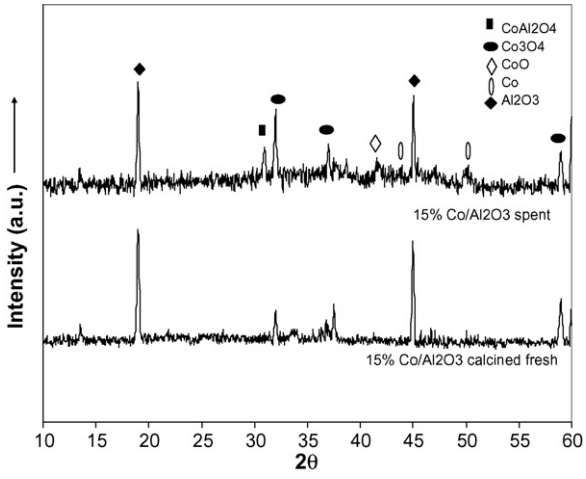

Fig. 1. XRD patterns of 15% Co/Al_2O_3 catalyst.

sites were available for these reactions that resulted in higher conversion. Beyond 15% Co metal loading, the ethanol conversion decreased significantly due to partial blockage of the pores of the support by metal. The activities of three catalysts evaluated as a function of contact-time is depicted in Fig. 3 at 773 K. The result indicated that, 15% Co catalyst had higher activity as compared to other catalysts.

3.3. Time on stream stability

To study the decline in activity for various cobalt-loaded catalysts, 20 h time-on-stream (TOS) tests were made at 773 K as shown in Fig. 4. The activity declined sharply initially up to a run time of 3 h and thereafter the decrease was gradual most probably due to some transient transformation to a stable form occurred under the reaction conditions in the catalyst. The 10 and 20% Co/Al_2O_3 catalysts deactivated rapidly compared to the 15% Co/Al_2O_3 catalyst. Carbon deposited on Co/Al_2O_3

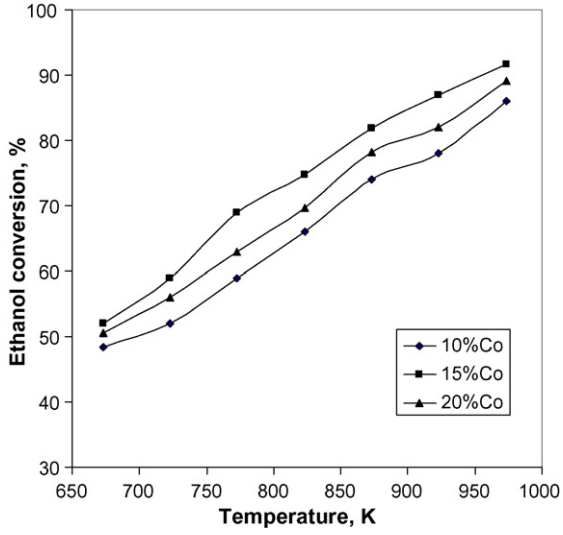

Fig. 2. Comparison of catalytic activity as a function of temperature for different Co/Al_2O_3 catalysts (W/F = 17 kg cat./(mol/s), S/E = 3 molar ratio).

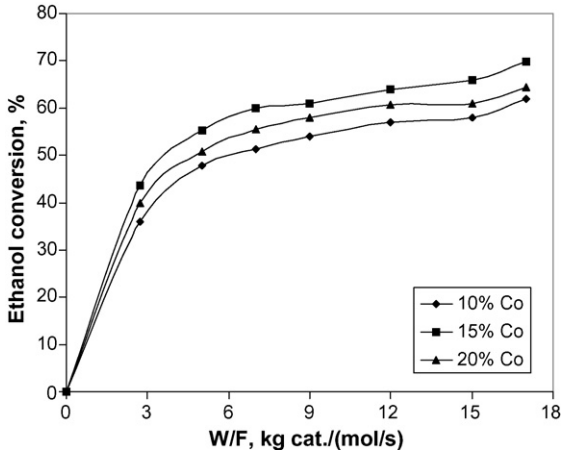

Fig. 3. Comparison of catalytic activity as a function of contact-time for different Co/Al_2O_3 catalysts (T = 773 K, S/E = 3 molar ratio).

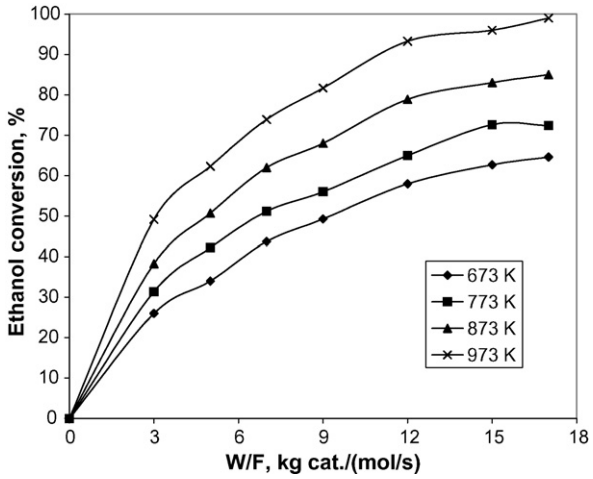

Fig. 5. Effect of contact-time on ethanol conversion for 15% Co/Al_2O_3 catalyst at different temperatures and S/E = 3 molar ratio.

catalysts could be due to the acid sites of alumina promoting the decomposition of ethanol molecules.

3.4. Effect of temperature

Based on the performance of catalysts for higher hydrogen selectivity and low deactivation rate, 15% Co/Al_2O_3 catalyst was chosen for further studies. Fig. 5 shows the effect of contact-time on conversion at different temperatures. Ethanol conversion increased as temperature was increased at all contact-times. The product composition (moles of product *i*/total moles of products) obtained with 15% Co/Al_2O_3 catalyst at different temperatures with contact-time 17 kg cat./(mol/s) is shown in Fig. 6. More than 70% of hydrogen could be achieved at temperature 773 K, which is well in agreement with the published literature [11]. However, the results were in contrast with the literature in the case of formation of ethylene. No ethylene was detected on Co/Al_2O_3 catalyst at a temperature more than 673 K.

Llorca et al. [15] reported that at low ethanol conversions formation of acetaldehyde takes place by dehydrogenation of ethanol over Co/ZnO catalyst it was due to basic properties of ZnO [15,16]; subsequently, the specific redox characteristics of ZnO contributed the steam reforming reaction at high ethanol conversion at which there was no acetaldehyde in the product stream. Homs et al. [17] observed no acetaldehyde at higher ethanol conversion over Ni/ZnO catalyst. The studies have shown that the concentration of acetaldehyde in final product stream depends upon the type of catalyst and support [10,11,15–19]. In present study over Co/Al_2O_3 catalyst, acetaldehyde was formed in trace form and ranged from 0.05 to 0.1% (mol) in product stream when ethanol conversion ranging from 10 to 40%. At ethanol conversion more than 40%, no acetaldehyde was observed with Co/Al_2O_3 catalysts. Therefore, in the results of kinetic studies, we neglected the formation of acetaldehyde. The effect of temperature on product selectivity and yield were studied at constant contact-time (17 kg cat./(mol/s)) and S/E ratio at 3. The variation in product selectivity (moles of product *i*/moles of ethanol converted) at different temperatures is presented in Fig. 7. The selectivity of CO and CH_4 increased progressively with temperature whereas selectivity of H_2 and CO_2 passed through maxima. A maximum selectivity was obtained at temperature 773 K. These

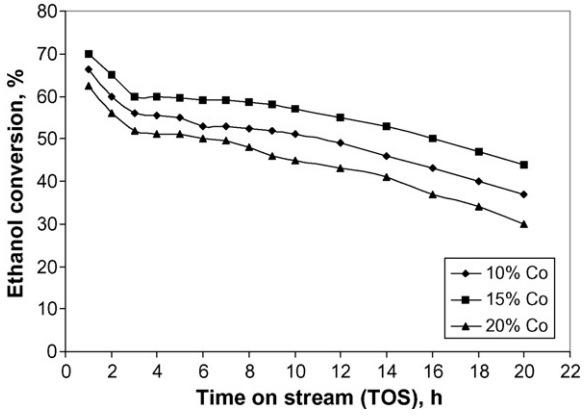

Fig. 4. Time-on-stream test for different Co/Al_2O_3 catalysts (T = 773 K, W/F = 17 kg cat./(mol/s), S/E = 3 molar ratio).

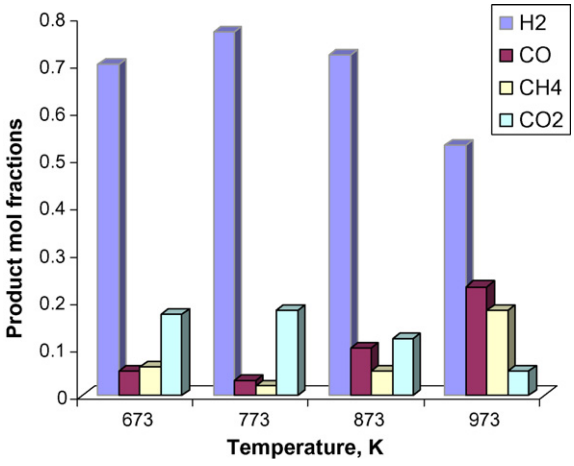

Fig. 6. Temperature evolution of reaction products over 15% Co/Al_2O_3 catalyst (W/F = 17 kg cat./(mol/s), S/E = 3 molar ratio).

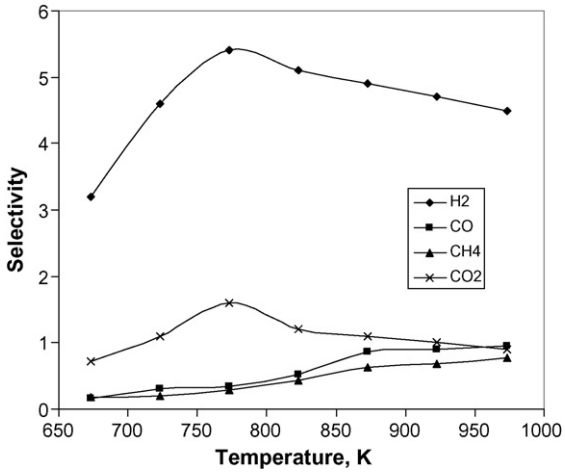

Fig. 7. Effect of temperature on product selectivity over 15% Co/Al_2O_3 catalyst (W/F = 17 kg cat./(mol/s), S/E = 3 molar ratio).

results indicate that temperature up to 773 K water gas shift reaction was favorable.

$$CO + H_2O \leftrightarrow CO_2 + H_2 \quad (2)$$

Due to this, H_2 selectivity increased significantly up to 773 K. The methane selectivity was low as compared to CO, which suggests the presence of methane reforming reaction

$$CH_4 + H_2O \leftrightarrow CO + 3H_2 \quad (3)$$

At temperature higher than 773 K, the rate of ethanol decomposition increase, which can be depicted from the marginal decrease in selectivity of H_2 and CO_2 while increase in selectivity of CO and CH_4.

3.5. Effect of contact-time

The ethanol conversion increased with contact-time, from 44 to 70% as the contact-time was varied from 3 to 17 kg cat./(mol/s) as shown in Fig. 5. The effect of contact-time on product selectivity as shown in Fig. 8 was studied at constant

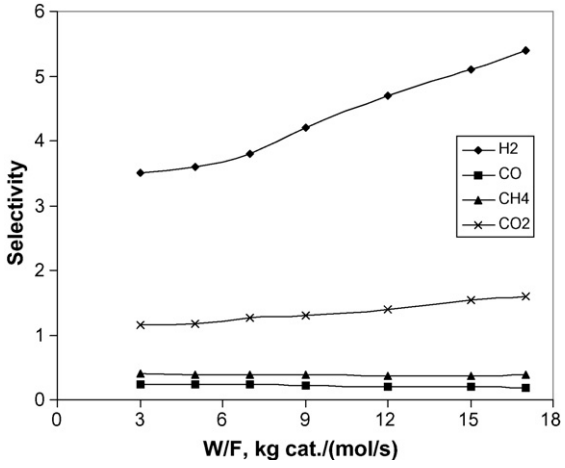

Fig. 8. Effect of contact-time on product selectivity over 15% Co/Al_2O_3 catalyst (T = 773 K, S/E = 3 molar ratio).

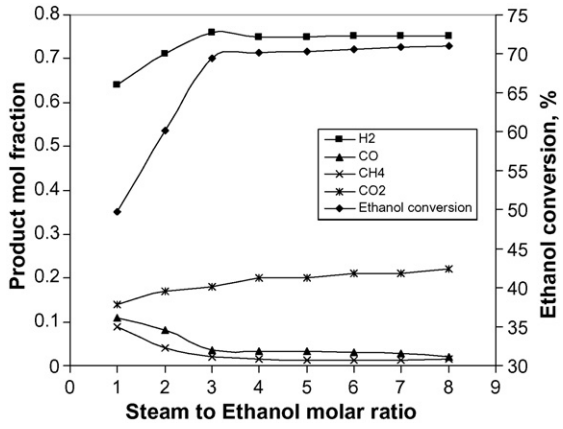

Fig. 9. Effect of steam to ethanol ratio on ethanol conversion and reaction products for 15% Co/Al_2O_3 catalyst (T = 773 K, W/F = 17 kg cat./(mol/s)).

temperature (773 K) and S/E ratio 3. The H_2 and CO_2 selectivity were found to be increased with increase in contact-time. This indicates that at higher contact-time, the water gas shift reaction and methanation reactions are instrumental. Thus, higher contact-time favors overall reforming reaction, where as the CH_4 and CO selectivity was nearly same with increase of contact-time suggesting that ethanol decomposition reaction may be responsible for the formation of both CO and CH_4, as it provides the same stoichiometric amounts of these products:

$$C_2H_5OH \leftrightarrow CH_4 + CO + H_2 \quad (4)$$

3.6. Effect of steam to ethanol molar ratio

The variation of ethanol conversion and product composition at different steam to ethanol (S/E) molar ratio is shown in Fig. 9. There was an increase in ethanol conversion with (S/E) molar ratio. SRE reaction (Eq. (1)) is dominating however the reactions (Eqs. (5) and (6)) are accelerated under this condition.

$$C_2H_5OH + H_2O \leftrightarrow 4H_2 + 2CO \quad (5)$$

$$C_2H_5OH \leftrightarrow CH_4 + CO + H_2 \quad (6)$$

While at high steam to ethanol ratio (≥2), the reactions (Eqs. (5) and (6)) suppressed highly due to excess availability of water. The following reactions accelerate along with SRE reaction (Eq. (1)).

$$CO + H_2O \leftrightarrow CO_2 + H_2 \quad (7)$$

$$CH_4 + H_2O \leftrightarrow CO + 3H_2 \quad (8)$$

Therefore, results showed the higher S/E molar ratio (≥2) is favorable for higher ethanol conversion and hydrogen formation, and for suppressing the CO concentration in product stream. The optimum (S/E) ratio can be recommended as 3 because further increase of (S/E) molar ratio neither increases ethanol conversion nor reduces CO formation significantly; instead, it increases reactor load and dilutes the product stream.

3.7. Kinetics study

Catalytic steam reforming of ethanol over Co/Al_2O_3 catalyst produces hydrogen and carbon dioxide primarily, with small amount of carbon monoxide and methane. The main reactions that occur with this catalyst are steam reforming, water gas shift and ethanol decomposition reactions:

$$C_2H_5OH + 3H_2O \leftrightarrow 6H_2 + 2CO_2 \quad \text{(SRE)} \tag{9}$$

$$C_2H_5OH \leftrightarrow CO + CH_4 + H_2 \quad \text{(ED)} \tag{10}$$

$$CO + H_2O \leftrightarrow CO_2 + H_2 \quad \text{(WGS)} \tag{11}$$

It is important to consider all the above three reactions viz., ethanol reforming, decomposition and water gas shift reactions simultaneously while developing the comprehensive model for steam reforming of ethanol process. In the absence of water, significant amount of methane was formed with the negligible CO_2. As soon as water vapor was supplied to the system, there was an inversion of the CH_4/CO_2 relative distribution. Furthermore, CO formation was also observed during the reforming of ethanol in the presence of water. These results confirmed that methane was mainly produced by the ethanol decomposition. Therefore, in order to model the variation in partial pressure of CO and CH_4, we consider the decomposition reaction and WGS reactions in the kinetic model of SRE process.

3.7.1. Reaction mechanism and kinetic model

There are different pathways suggested for the ethanol steam reforming [11,15,18,20–26]. The main reaction mechanism involves dehydrogenation or dehydration reactions. Dehydration reactions produce intermediate products such as ethylene, which is easily transformed into carbon that is deposited on the active phase producing the catalyst poisoning. In the dehydrogenation step ethanol converted to the acetaldehyde which further transformed in to the reforming products. In the present study, hydrogen, carbon dioxide, carbon monoxide and methane were present in the product distribution. The traces of acetaldehyde also observed at low ethanol conversion. This fact indicates that cobalt favors dehydrogenation reaction. Cavallaro and Freni [9] reported that at temperature higher than 648 K, no traces of intermediate products such as acetic acid, acetaldehyde and ethyl acetate were observed. These compounds were produced at temperature below 648 K when the hydrogen and carbon dioxide selectivity is very low. Diagne et al. [26] proposed the dehydrogenation of ethanol to ethoxy, which subsequently transformed in to acetaldehyde. The formation of intermediates in the proposed reaction mechanism has been confirmed with the literature. In the DRIFT-mass spectroscopy study of Llorca et al. [27] reported the formation of surface ethoxy species over Co/ZnO catalyst. The physisorbed acetaldehyde also observed over the catalyst. There were two bands of acetate species and one band of acetyl species was confirmed. In the microcalometric and infrared studies, Guil et al. [16] reported that steam reforming of ethanol proceeds via formation of intermediate acetaldehyde. Then, acetaldehyde subsequently transformed in to adsorbed methane and carbon monoxide. They also confirmed through calorimetric curves that ethanol and acetaldehyde adsorbed on same sites over Co/ZnO catalyst under SRE reaction conditions. In the development of the kinetic model, the rate-determining steps for SRE, WGS and ED are taken as dehydrogenation of adsorbed ethoxy, decomposition of an intermediate formate species and decomposition of acetaldehyde, respectively. Based on available literature and product analysis, following reaction steps were considered during SRE process.

$$2S_1 + CH_3CH_2OH\,(g) \overset{k_{1,-1}}{\longleftrightarrow} CH_3CH_2O^{(1)} + H^{(1)} \tag{12}$$

$$S_1 + CH_3CH_2O^{(1)} \overset{k_{2,-2}}{\longleftrightarrow} CH_3CHO^{(1)} + H^{(1)} \quad \text{(RDS : SRE)} \tag{13}$$

$$2S_1 + H_2O\,(g) \overset{k_{3,-3}}{\longleftrightarrow} OH^{(1)} + H^{(1)} \tag{14}$$

$$CH_3CHO^{(1)} + H^{(1)} \overset{k_{4,-4}}{\longleftrightarrow} CH_3{}^{(1)} + HCHO^{(1)} \tag{15}$$

$$CH_3{}^{(1)} + OH^{(1)} \overset{k_{5,-5}}{\longleftrightarrow} CH_3OH^{(1)} + S_1 \tag{16}$$

$$CH_3OH^{(1)} \overset{k_{6,-6}}{\longleftrightarrow} CH_3O^{(1)} + OH^{(1)} \tag{17}$$

$$CH_3O^{(1)} + S_1 \overset{k_{7,-7}}{\longleftrightarrow} HCHO^{(1)} + H^{(1)} \tag{18}$$

$$HCHO^{(1)} + OH^{(1)} \overset{k_{8,-8}}{\longleftrightarrow} HCOOH^{(1)} + H^{(1)} \tag{19}$$

$$2S_1 + HCOOH^{(1)} \overset{k_{9,-9}}{\longleftrightarrow} CO_2{}^{(1)} + H^{(1)} \tag{20}$$

$$CO_2{}^{(1)} \overset{k_{10,-10}}{\longleftrightarrow} CO_2\,(g) + S_1 \tag{21}$$

$$2H^{(1)} \overset{k_{11,-11}}{\longleftrightarrow} H_2\,(g) + 2S_1 \tag{22}$$

Additional steps in WGS

$$2S_1 + HCOOH^{(1)} \overset{k_{12,-12}}{\longleftrightarrow} HCOO^{(1)} + H^{(1)} \tag{23}$$

$$S_1 + HCOO^{(1)} \overset{k_{13,-13}}{\longleftrightarrow} CO^{(1)} + OH^{(1)} \quad \text{(RDS : WGS)} \tag{24}$$

$$CO^{(1)} \overset{k_{14,-14}}{\longleftrightarrow} CO\,(g) + S_1 \tag{25}$$

$$S_1 + HCOO^{(1)} \overset{k_{15,-15}}{\longleftrightarrow} CO_2{}^{(1)} + H^{(1)} \tag{26}$$

Additional steps in ED

$$S_1 + CH_3CHO^{(1)} \overset{k_{16,-16}}{\longleftrightarrow} CH_4{}^{(1)} + CO^{(1)} \quad \text{(RDS : ED)} \tag{27}$$

$$CH_4{}^{(1)} \overset{k_{17,-17}}{\longleftrightarrow} CH_4\,(g) + S_1 \tag{28}$$

Except for the rate-determining steps, rate of other reactions can be assumed to be at equilibrium, and so the site concentration of various intermediate species formed in the equation were written using Langmuir–Hinshelwood approach. The equilibrium constants are written as following:

$$K_1 = \frac{[CH_3CH_2O^{(1)}][H^{(1)}]}{p_{C_2H_5OH} C_{S1}^2} \tag{29}$$

$$K_3 = \frac{[OH^{(1)}][H^{(1)}]}{p_{H_2O} C_{S1}^2} \tag{30}$$

$$K_4 = \frac{[CH_3{}^{(1)}][HCHO^{(1)}]}{[CH_3CHO^{(1)}][H^{(1)}]} \quad (31)$$

$$K_5 = \frac{[CH_3OH^{(1)}]C_{S1}}{[CH_3{}^{(1)}][OH^{(1)}]} \quad (32)$$

$$K_6 = \frac{[CH_3O^{(1)}][OH^{(1)}]}{[CH_3OH^{(1)}]C_{S1}} \quad (33)$$

$$K_7 = \frac{[HCHO^{(1)}][H^{(1)}]}{[CH_3O^{(1)}]C_{S1}} \quad (34)$$

$$K_8 = \frac{[HCOOH^{(1)}][H^{(1)}]}{[HCHO^{(1)}][OH^{(1)}]} \quad (35)$$

$$K_9 = \frac{[CO_2{}^{(1)}][H^{(1)}]}{[HCOOH^{(1)}]C_{S1}^2} \quad (36)$$

$$K_{10} = \frac{P_{CO_2}C_{S1}}{[CO_2{}^{(1)}]} \quad (37)$$

$$K_{11} = \frac{P_{H_2}C_{S1}^2}{[H^{(1)}]^2} \quad (38)$$

$$K_{12} = \frac{[HCOO^{(1)}][H^{(1)}]}{[HCOOH^{(1)}]C_{S1}^2} \quad (39)$$

$$K_{14} = \frac{P_{CO}C_{S1}}{[CO^{(1)}]} \quad (40)$$

$$K_{15} = \frac{[CO_2{}^{(1)}][H^{(1)}]}{[HCOO^{(1)}]C_{S1}} \quad (41)$$

Using above relations, the concentrations of all the intermediate products were derived in the form of measurable partial pressure quantities. The rate equations have been developed by taking the rate-determining steps (Eqs. (13), (24) and (27)) of SRE, WGS and ED reactions, respectively, into consideration.

$$r_{SRE} = k_r[CH_3CH_2O^{(1)}]C_{S1} - k_{-r}[CH_3CHO^{(1)}][H^{(1)}] \quad (42)$$

$$r_{WGS} = k_w[HCOO^{(1)}]C_{S1} - k_{-w}[OH^{(1)}][CO^{(1)}] \quad (43)$$

$$r_{ED} = k_D[CH_3CHO^{(1)}]C_{S1} - k_{-D}[CH_4{}^{(1)}][CO^{(1)}] \quad (44)$$

The final rate expressions are given in Table 2. During the kinetic experiments, the amounts of H_2, CO and CO_2 formed were determined at various conditions. In order to model the experimental data, the rate expressions for each individual reaction were combined to get an overall rate expression for different species. Since the rates of different species are interrelated by stoichiometry, the rate of each individual species was calculated. The pressure drop inside the bed was assumed to be negligible. The partial pressures of individual species comprising in rate expressions iteratively were calculated from mol fractions.

3.7.2. Estimation of kinetic model parameters

There are eight equilibrium constants and three rate constants in rate expressions (Table 2). The temperature dependences of each of these were estimated from Arrhenius and Vant Hoff expressions. For the estimation of the equilibrium constants, heat of adsorptions were taken from the literature and their entropies were determined using non-linear regression. The kinetic parameters were determined by minimizing the squared sum of the error between experimental and simulated data. The values of the parameters for optimal fit were determined using non-linear regression and are listed in Table 3. The kinetic model developed by Akande et al. [18] using Eley Rideal considering only stream reforming reaction. They have reported activation energy of reforming reaction very low 4.03–7.56 kJ/mol for different models. The comparison between model predicted methanol conversion and experimental conversion at various temperatures is shown in Fig. 10. In the range of experiments, the model predicted conversion was well in match with the experimental data at all temperatures. The model predicted and experimentally observed variation of product mol fractions with the contact-time depicted in Fig. 11. The correlation coefficient (R^2) value for all cases was above 0.95, indicating that the error between experimental and simulated results is within statistically permissible limits. The product selectivity of H_2, CO, CH_4 and CO_2 are found to be non-zero at zero conversion values indicating

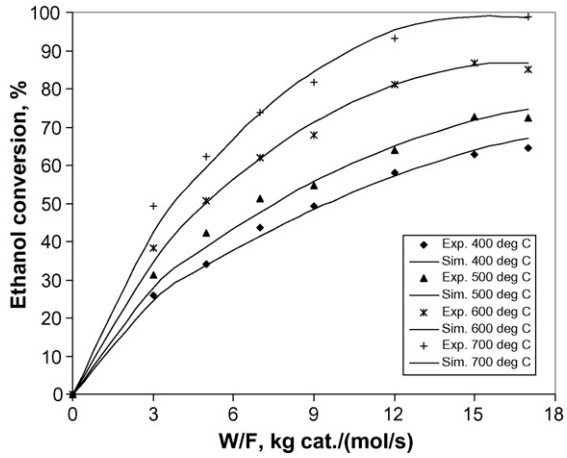

Fig. 10. Simulated and experimental ethanol conversion vs. contact-time for 15% Co/Al_2O_3 catalyst at different temperatures and S/E = 3 molar ratio.

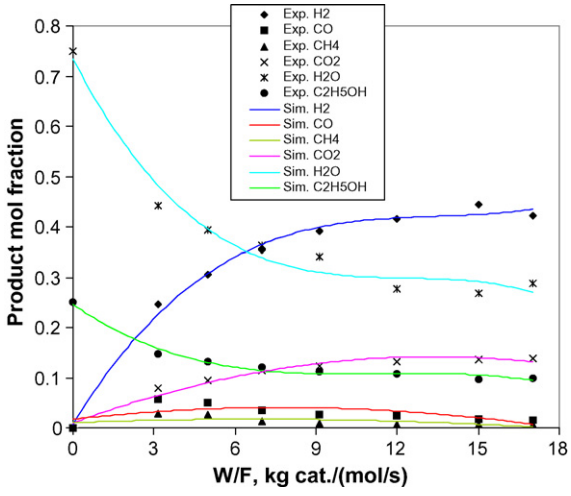

Fig. 11. Experimental and simulated results of product mol fractions for 15% Co/Al_2O_3 catalyst (T = 773 K, S/E = 3 molar ratio).

Table 2
Kinetic model rate expressions of ethanol steam reforming process.

Reaction	Rate expressions
SRE	$r_{\mathrm{SRE}} = \dfrac{k_{\mathrm{r}} K_{\mathrm{CH_3CH_2O^{(1)}}} \left(\dfrac{p_{\mathrm{C_2H_5OH}}}{P_{H_2}^{\frac{1}{2}}} \right) \left[1 - \dfrac{P_{\mathrm{CO_2}}^2 P_{\mathrm{H_2}}^4}{K_{\mathrm{r}}^* p_{\mathrm{C_2H_5OH}} P_{\mathrm{H_2O}}^2} \right]}{1 + K_{\mathrm{CO_2^{(1)}}} P_{\mathrm{CO_2}} + K_{\mathrm{CO^{(1)}}} P_{\mathrm{CO}} + K_{\mathrm{CH_4^{(1)}}} P_{\mathrm{CH_4}} + K_{\mathrm{HCOO^{(1)}}} P_{\mathrm{CO_2}} P_{H_2}^{\frac{1}{2}} + K_{\mathrm{H_2^{(1)}}} P_{H_2}^{\frac{1}{2}} + \dfrac{K_{\mathrm{CH_3CHO^{(1)}}} P_{\mathrm{CO_2}}^2 P_{\mathrm{H_2}}^5}{P_{\mathrm{H_2O}}^3} + \dfrac{K_{\mathrm{CH_3CH_2O^{(1)}}} p_{\mathrm{C_2H_5OH}}}{P_{\mathrm{H_2}}^{1/2}} + \dfrac{K_{\mathrm{OH^{(1)}}} P_{\mathrm{H_2O}}}{P_{\mathrm{H_2}}^{1/2}}} C_{\mathrm{S1}}^{\mathrm{T}^2}$ where, $K_{\mathrm{r}}^* = \dfrac{K_{\mathrm{CH_3CH_2O^{(1)}}} \left(\dfrac{k_{\mathrm{r}}}{k_{-\mathrm{r}}} \right)}{K_{\mathrm{CH_3CHO^{(1)}}} K_{\mathrm{H_2^{(1)}}}}$
WGS	$r_{\mathrm{WGS}} = \dfrac{k_{\mathrm{w}} K_{\mathrm{HCOO^{(1)}}} P_{\mathrm{CO_2}} \left[1 - \left(\dfrac{p_{\mathrm{H_2O}} p_{\mathrm{CO}}}{K_{\mathrm{w}}^* P_{\mathrm{H_2}} P_{\mathrm{CO_2}}} \right) \right]}{1 + K_{\mathrm{CO_2^{(1)}}} P_{\mathrm{CO_2}} + K_{\mathrm{CO^{(1)}}} P_{\mathrm{CO}} + K_{\mathrm{CH_4^{(1)}}} P_{\mathrm{CH_4}} + K_{\mathrm{HCOO^{(1)}}} P_{\mathrm{CO_2}} P_{H_2}^{\frac{1}{2}} + K_{\mathrm{H_2^{(1)}}} P_{H_2}^{\frac{1}{2}} + \dfrac{K_{\mathrm{CH_3CHO^{(1)}}} P_{\mathrm{CO_2}}^2 P_{\mathrm{H_2}}^5}{P_{\mathrm{H_2O}}^3} + \dfrac{K_{\mathrm{CH_3CH_2O^{(1)}}} p_{\mathrm{C_2H_5OH}}}{P_{\mathrm{H_2}}^{1/2}} + \dfrac{K_{\mathrm{OH^{(1)}}} P_{\mathrm{H_2O}}}{P_{\mathrm{H_2}}^{1/2}}} C_{\mathrm{S1}}^{\mathrm{T}^2}$ where, $K_{\mathrm{w}}^* = \dfrac{K_{\mathrm{HCOO^{(1)}}} \left(\dfrac{k_{\mathrm{w}}}{k_{-\mathrm{w}}} \right)}{K_{\mathrm{OH^{(1)}}} K_{\mathrm{CO^{(1)}}}}$
ED	$r_{\mathrm{ED}} = \dfrac{k_{\mathrm{D}} K_{\mathrm{CH_3CHO^{(1)}}} \left(\dfrac{P_{\mathrm{CO_2}}^2 P_{\mathrm{H_2}}^3}{P_{\mathrm{H_2O}}^2} \right) \left[1 - \dfrac{P_{\mathrm{H_2O}}^2 P_{\mathrm{CH_4}} P_{\mathrm{CO}}}{K_{\mathrm{D}}^* P_{\mathrm{CO_2}}^2 P_{\mathrm{H_2}}^3} \right]}{1 + K_{\mathrm{CO_2^{(1)}}} P_{\mathrm{CO_2}} + K_{\mathrm{CO^{(1)}}} P_{\mathrm{CO}} + K_{\mathrm{CH_4^{(1)}}} P_{\mathrm{CH_4}} + K_{\mathrm{HCOO^{(1)}}} P_{\mathrm{CO_2}} P_{\mathrm{H_2}}^{1/2} + K_{\mathrm{H_2^{(1)}}} P_{\mathrm{H_2}}^{1/2} + \dfrac{K_{\mathrm{CH_3CHO^{(1)}}} P_{\mathrm{CO_2}}^2 P_{\mathrm{H_2}}^5}{P_{\mathrm{H_2O}}^3} + \dfrac{K_{\mathrm{CH_3CH_2O^{(1)}}} p_{\mathrm{C_2H_5OH}}}{P_{\mathrm{H_2}}^{1/2}} + \dfrac{K_{\mathrm{OH^{(1)}}} P_{\mathrm{H_2O}}}{P_{\mathrm{H_2}}^{1/2}}} C_{\mathrm{S1}}^{\mathrm{T}^2}$ where, $K_{\mathrm{D}}^* = \dfrac{K_{\mathrm{CH_3CHO^{(1)}}} \left(\dfrac{k_{\mathrm{D}}}{k_{-\mathrm{D}}} \right)}{K_{\mathrm{CH_4^{(1)}}} K_{\mathrm{CO^{(1)}}}}$

Table 3
Final values of parameters estimated after regression

Parameters	k_i^{∞} (m^2/(mol s))	E_i (kJ/mol)	ΔS_i (J/(mol K))
k_r	1.16E + 20	82.7	
k_w	4.64E + 16	43.6	
k_D	4.46E + 19	71.3	
$\Delta S_{CH_3CH_2O^{(1)}}$			−34.6
$\Delta S_{CO_2{}^{(1)}}$			−47.5
$\Delta S_{CO^{(1)}}$			−49.2
$\Delta S_{CH_4{}^{(1)}}$			−58.3
$\Delta S_{HCOO^{(1)}}$			112.3
$\Delta S_{H_2{}^{(1)}}$			−101.5
$\Delta S_{CH_3CHO^{(1)}}$			−38.7
$\Delta S_{OH^{(1)}}$			−44.6
C_{S1}^{T} (mol/m^2)	1.04E − 21		

that all these products are the primary products of the reactions. Hence, it can be concluded that the steam reforming reaction and decomposition reaction are taking place simultaneously in the reactor. Also, the CO selectivity is decreasing with conversion; it shows that WGS reaction is also taking place in the reactor. Hence, the kinetic model consisting of the SRE, WGS and ED reactions as the main reactions, developed in present study satisfies the experimental data.

4. Conclusion

The 15% Co/Al_2O_3 catalyst prepared by wet impregnation technique was found effective for the production of hydrogen by steam reforming of ethanol. Ethanol conversion increases with increase in temperature, contact-time and steam to ethanol molar ratio. The H_2 concentration was maximum at 773 K and W/F = 17 kg cat./(mol/s) and S/E molar ratio 3. The optimum operating conditions in order to achieve H_2 rich product stream with minimum CO and CH_4 suggested for steam reforming of ethanol are, temperature 773 K, S/E molar ratio = 3–5 and contact-time (W/F) 15–17 kg cat./(mol/s). Above 773 K, ethanol decomposition reaction favors which decreases the hydrogen selectivity. The mechanistic kinetic model incorporating the effect of process variables developed was able to describe the experimental kinetics data. The results indicated that the model fits reasonably well to the experimental result at all temperature, contact-time and conversion level.

References

[1] S. Freni, S. Cavallaro, N. Mondello, L. Spadaro, F. Frusteri, J. Power Sources 108 (2002) 53–57.
[2] V. Agarwal, S. Patel, K.K. Pant, Appl. Catal. A 279 (2005) 155–164.
[3] S. Patel, K.K. Pant, J. Porous Mater. 13 (2006) 381–386.
[4] P.D. Vaidya, A.E. Rodrigues, Chem. Eng. J. 117 (2006) 39–49.
[5] M.N. Barroso, M.F. Gomez, L.A. Arrua, M.C. Abello, Appl. Catal. A 304 (2006) 116–123.
[6] J. Sun, X. Qiu, F. Wu, W. Zhu, W. Wang, S. Hao, Int. J. Hydrogen Energy 29 (2004) 1075–1081.
[7] K. Vasudeva, N. Mitra, P. Umasankar, S.C. Dhingra, Int. J. Hydrogen Energy 21 (1996) 13–18.
[8] L. Garcia, R. French, S. Czernik, E. Chornet, Appl. Catal. A 201 (2000) 225–239.
[9] S. Cavallaro, S. Freni, Int. J. Hydrogen Energy 21 (1996) 465–469.
[10] F. Haga, T. Nakajima, H. Miya, S. Mishima, Catal. Lett. 48 (1997) 223–227.
[11] M.S. Batista, R.K.S. Santos, E.M. Assaf, J.M. Assaf, E.A. Ticianelli, J. Power Sources 124 (2003) 99–103.
[12] R.O. Idem, N.N. Bakhshi, Chem. Eng. Sci. 51 (1996) 3697–3708.
[13] G.F. Froment, K.B. Bischoff, Chemical Reactor Analysis and Design, second ed., Wiley, New York, 1990.
[14] D.E. Mears, Tests for transport limitations in experimental catalytic reactors, Ind. Eng. Chem. Proc. Des. Dev. 10 (1971) 541–547.
[15] J. Llorca, P.R. de la Piscina, J. Dalmon, J. Sales, N. Homs, Appl. Catal. B 43 (2003) 355–369.
[16] J.M. Guil, N. Homs, J. Llorca, P.R. de la Piscina, J. Phys. Chem. B 109 (2005) 10813–10819.
[17] N. Homs, J. Llorca, P.R. de la Piscina, Catal. Today 116 (2006) 361–366.
[18] A. Akande, A. Aboudheir, R. Idem, A. Dalai, Int. J. Hydrogen Energy 31 (2006) 1707–1715.
[19] A. Casanovas, J. Llorca, N. Homs, J.L.G. Fierro, P.R. de la Piscina, J. Mol. Catal. A 250 (2006) 44–49.
[20] A.N. Fatsikostas, X.E. Verykios, J. Catal. 225 (2004) 439–452.
[21] P.Y. Sheng, G.A. Bowmaker, H. Idriss, Appl. Catal. A 261 (2004) 171–181.
[22] S.R. Segal, K.A. Carrado, C.L. Marshall, K.B. Anderson, Appl. Catal. A 248 (2003) 33–45.
[23] J. Rasko, A. Hancz, A. Erdohelyi, Appl. Catal. A 269 (2004) 13–25.
[24] J. Rasko, M. Domok, K. Baan, A. Erdohelyi, Appl. Catal. A 299 (2006) 202–211.
[25] M. Benito, J.L. Sanz, R. Isabel, R. Padilla, R. Arjona, L. Daza, J. Power Sources 152 (2005) 11–17.
[26] C. Diagne, H. Idriss, A. Kiennemann, Catal. Commun. 3 (2002) 565–571.
[27] J. Llorca, N. Homs, P.R. de la Piscina, J. Catal. 227 (2004) 556–560.